

Primary hematopoietic cells from DBA patients with mutations in *RPL11* and *RPS19* genes exhibit distinct erythroid phenotype *in vitro*

H Moniz^{1,2,3}, M Gastou^{1,2,3}, T Leblanc⁴, C Hurtaud^{1,2,3}, A Crétien^{1,2,3}, Y Lécluse^{2,3}, H Raslova^{1,2,3}, J Larghero^{5,6}, L Croisille⁷, M Faubladiere^{8,9}, O Bluteau^{1,2,3}, L Lordier^{1,2,3}, G Tchernia¹⁰, W Vainchenker^{1,2,3}, N Mohandas¹¹, L Da Costa^{*,1,6,12} and on behalf of the DBA group of Société d'Hématologie et d'Immunologie pédiatrique (SHIP)

Diamond-Blackfan anemia (DBA) is caused by aberrant ribosomal biogenesis due to ribosomal protein (RP) gene mutations. To develop mechanistic understanding of DBA pathogenesis, we studied CD34⁺ cells from peripheral blood of DBA patients carrying *RPL11* and *RPS19* ribosomal gene mutations and determined their ability to undergo erythroid differentiation *in vitro*. *RPS19* mutations induced a decrease in proliferation of progenitor cells, but the terminal erythroid differentiation was normal with little or no apoptosis. This phenotype was related to a G₀/G₁ cell cycle arrest associated with activation of the p53 pathway. In marked contrast, *RPL11* mutations led to a dramatic decrease in progenitor cell proliferation and a delayed erythroid differentiation with a marked increase in apoptosis and G₀/G₁ cell cycle arrest with activation of p53. Infection of cord blood CD34⁺ cells with specific short hairpin (sh) RNAs against *RPS19* or *RPL11* recapitulated the two distinct phenotypes in concordance with findings from primary cells. In both cases, the phenotype has been reverted by shRNA p53 knockdown. These results show that p53 pathway activation has an important role in pathogenesis of DBA and can be independent of the *RPL11* pathway. These findings shed new insights into the pathogenesis of DBA.

Cell Death and Disease (2012) 3, e356; doi:10.1038/cddis.2012.88; published online 26 July 2012

Subject Category: Immunity

Diamond Blackfan anemia (DBA) is a rare congenital disorder characterized by a moderate to severe anemia, in conjunction with erythroblastopenia (absence or <5% of erythroid precursors) in an otherwise normocellular bone marrow. In 40% of DBA cases, various malformations, mostly in the cephalic area, thumbs and upper limbs, are observed.^{1,2} More than 60% of DBA patients respond to steroid treatment. The steroid-resistant DBA patients are treated with regular transfusions in conjunction with iron chelation therapy. The only curative treatment is hematopoietic stem cell transplantation.^{1–3}

Mutations in gene encoding the ribosomal protein S19 gene (*RPS19*) were the first to be identified in DBA and 25% of DBA patients carry mutations in this gene.⁴ Recently, mutations in genes encoding other RPs of both the small and the large subunits have been identified in DBA patients: *RPS24* (2%),⁵ *RPS17* (<1%),⁶ *RPL5* (7%),^{7–9} *RPL11* (5%),^{7–9} *RPL36*

(<1%),⁸ *RPS7* (<1%),⁸ *RPS27a* (<1%),⁸ *RPS15* (<1%),⁸ *RPL35a* (3%),¹⁰ *RPS10* (3%)¹¹ and *RPS26* (7%).¹¹ More recently, large deletions in *RPS19*, *RPS17*, *RPS26* and *RPL35a* genes have been identified in 17% of DBA cases.¹² Thus, ≈75% of the DBA patients exhibit a *RP* gene mutation or deletion. The remaining 25% may carry a mutation in the non-coding region of a *RP* gene or in other gene(s) yet to be defined. Mutations identified in *RPS19*, *RPS10*, *RPS24* and *RPS26*, as well as reduced expression of several RPs by small interfering RNAs, result in defective ribosomal biogenesis at different stages of ribosomal RNA (rRNA) maturation.^{11,13–16} Defective ribosomal biogenesis appears to be the major cause of DBA.¹⁷

Animal models^{18–23} have begun to provide some mechanistic insights into DBA pathogenesis. Large scale chemical mutagenesis screen for dark skin phenotype identified a mutation in *rps19* or *rsp20* genes (*Dsk3*^{+/-} and *Dsk4*^{+/-},

¹INSERM UMR U1009, Institut Gustave Roussy, Villejuif, France; ²Université Paris-Sud, UMR1009, Institut Gustave Roussy, Villejuif, France; ³Institut Gustave Roussy, UMR1009, Villejuif, France; ⁴AP-HP, Service d'Onco-Hématologie pédiatrique, Hôpital Robert Debré, Paris, France; ⁵AP-HP, Hôpital Saint-Louis, Unité de Thérapie cellulaire et CIC de Biothérapie, Paris, France; ⁶Université Paris VII-Denis Diderot, Sorbonne Paris Cité, Paris, France; ⁷AP-HP, Laboratoire d'Hématologie, Hôpital Bicêtre, Le Kremlin-Bicêtre, Paris, France; ⁸CNRS, UMR5099, Laboratoire de Biologie moléculaire des eucaryotes, Université Paul Sabatier, Toulouse, France; ⁹Université Paul Sabatier, UMR5099, Laboratoire de Biologie moléculaire des eucaryotes, Toulouse, France; ¹⁰Centre de dépistage de la drépanocytose, Paris, France; ¹¹New York Blood Center, New York, NY, USA and ¹²AP-HP, Service d'Hématologie Biologique, Hôpital Robert Debré, Paris, France

*Corresponding author: L Da Costa, AP-HP, Hematology Laboratory, Robert Debré Hospital, 48 Boulevard Sérurier, Paris, Cedex 75935, France. Tel: +33 1 40 03 41 66; Fax: +33 1 40 03 47 95. E-mail: lydie.dacosta@rdh.aphp.fr

Keywords: DBA; *RPS19*; *RPL11*; p53; apoptosis; cell cycle

Abbreviations: DBA, Diamond-Blackfan anemia; RP, ribosomal protein; rRNA, ribosomal RNA; MDM-2, murine double minute 2; HDM-2, human double minute 2; GFP, green fluorescent protein; MOI, multiplicity of infection; EPO, erythropoietin; FBS, fetal bovine serum; SCF, stem cell factor; IL-3, interleukin-3; IMDM, Iscove's modified Dulbecco's media; PE, phycoerythrin; APC, allophycocyanin; GPA, glycophorin a; QRT-PCR, quantitative reverse transcriptase-PCR; HPRT, hypoxanthine guanine phosphoribosyl transferase; GAPDH, glyceraldehyde-3-phosphate dehydrogenase; TBST, Tris-buffered saline with Tween 20; PARP, poly (ADP-ribose) polymerase; ECL, enhanced chemiluminescent

Received 19.4.12; revised 25.5.12; accepted 29.5.12; Edited by G Raschella

respectively)²¹ in association with two clinical features associated with DBA, growth retardation and a modest decrease in red cell count. In this model, p53 expression level was increased and the phenotype was rescued following inhibition of p53. The p53 pathway was also implicated in Zebrafish morpholino models of RPS19 and RPL11, which show a delay in erythroid differentiation.^{18,19,23} Furthermore, Fumagalli *et al.*²⁴ have shown that depletion of RPS6, RPS23 and RPL7a in hepatocytes leads to the activation of p53 pathway with increased expression of RPL11 suppressing the murine double minute 2 (MDM-2) E3 ligase activity against p53.

To further understand the mechanistic basis of DBA, we explored the ability of primary circulating CD34⁺ cells of DBA patients with either RPS19 or RPL11 mutations to undergo *in vitro* erythroid differentiation. In parallel, we studied erythroid differentiation of normal human CD34⁺ cells infected with specific short hairpin (sh) RNA against RPS19 and RPL11. We show here that while RPS19 depletion decreases progenitor proliferation without affecting terminal erythroid differentiation, RPL11 depletion affects both progenitor cell proliferation and erythroid differentiation with marked apoptosis. Although the p53 pathway is involved in both situations, its role is more limited in RPS19-deficient samples. Thus, we identified two different erythroid differentiation phenotypes due to different ribosomal mutations that could account for erythroblastopenia, the main characteristic of DBA. Strikingly, p53 pathway was activated without increased RPL11 expression level in RPL11-mutated DBA patients or RPL11-depleted cord blood CD34⁺ cells implying that RPL11 is not necessary in p53 activation following RP depletion.

Results

Two different erythroid differentiation phenotypes in DBA depending on the specific RP defect. We compared the ability of CD34⁺ cells isolated from peripheral blood from DBA individuals with RPS19 ($n=12$) or RPL11 ($n=3$) mutations and CD34⁺ cells from healthy controls ($n=15$) to undergo terminal erythroid differentiation (Table 1). CD34⁺ cells were cultured either in two phases (7 day methylcellulose and then liquid culture for additional 5 days) or in a single phase (liquid culture over 12 days). At day 7 of the culture in methylcellulose, immunoblot analyses confirmed the decreased expression of RPS19 or RPL11 in DBA patients compared with healthy controls (Figure 1a), with RPL11 expression consistently decreasing to a greater extent than RPS19 expression. In liquid culture, we observed a decrease in cell amplification for all DBA patients irrespective of the mutational status. As illustrated in Figure 1b, this decrease was less pronounced from D0 to D7 for samples with RPS19 mutations than for samples with mutations in RPL11. This trend of decreased proliferation continued into later stages of culture (D7 to D10). Cytological examination of erythroid cell precursors generated did not show any significant abnormality when RPS19-mutant CD34⁺ cells were cultured ($n=12$) while immature and some apoptotic or necrotic cells were observed when RPL11-mutant CD34⁺ cells were cultured ($n=3$)

Table 1 Clinical and biological data of the DBA patients

DBA	Sex	Mode of inheritance	Age at diagnosis (month)	Hb at diagnosis (g/dl)	Absolute retic count (giga/l)	eADA (nmoles/min/mg)	Congenital malformations	Treatment at the time of the study	Genotype
1	F	Sporadic	NA	NA	NA	1.61	Hypogammaglobulinemia, short stature	IT	RPS19 ^{+/-}
2	F	Sporadic	3	5.6	NA	3.6	Short stature, prognatism, low hair implantation	T	RPS19 ^{+/-}
3	M	Sporadic	2	3.7	3	4.9	Epicanthus, low hair implantation	C	RPS19 ^{+/-}
4	F	Sporadic	3.5	3.7	4	0.86	Short stature, surdity, hip dysplasia	T	RPS19 ^{+/-}
5	M	Sporadic	NA	NA	NA	NA	Heart, bones, epilepsy, hydrocephaly	T	RPS19 ^{+/-}
6	F	Familial	2	5	<20	Normal	No	NA	RPS19 ^{+/-}
7	M	Familial	NA	NA	NA	NA	No	NA	RPS19 ^{+/-}
8	M	Sporadic	1.5	4.2	595	NA	No	T	RPS19 ^{+/-}
9	F	Sporadic	NA	4.5	NA	NA	No	T	RPS19 ^{+/-}
10	F	Sporadic	2	4.5	12.5	3	No	T	RPS19 ^{+/-}
11	F	Sporadic	1	3.9	4.56	NA	Growth retardation	IT	RPS19 ^{+/-}
12	F	Sporadic	2	4.2	2	NA	Diabetes, low implantation of the thumb	T	RPS19 ^{+/-}
13	M	Sporadic	Birth	9.5	15	4.93	Spina bifida, dysimmunity, triphalangeal thumb	C	RPL11 ^{+/-}
14	M	Sporadic	3	3.3	5	NA	Short stature, flat tenar	C	RPL11 ^{+/-}
15	M	Sporadic	1	6.4	9	6.15	No	T	RPL11 ^{+/-}

Abbreviations: C, corticosteroids; eADA, erythrocyte adenosine deaminase; F, female; IT, treatment independence; M, male; NA, not available; T, transfusions.

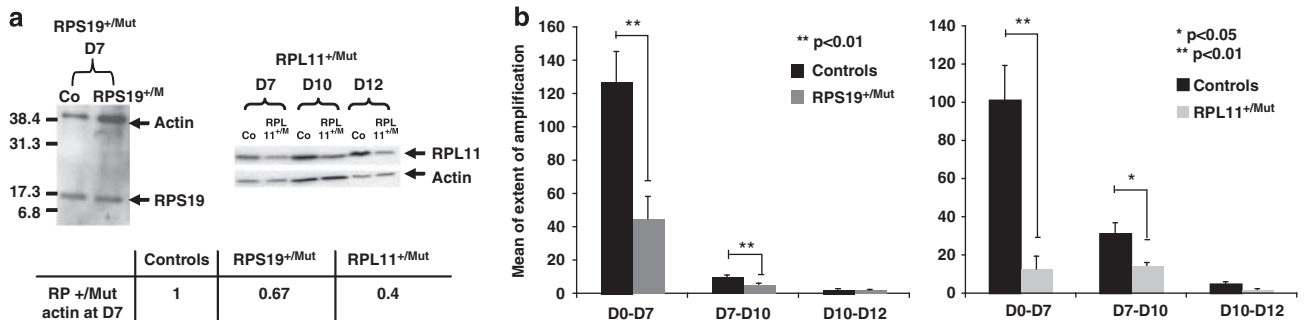


Figure 1 Erythroid proliferation is decreased to greater extent in DBA patients carrying mutations in *RPL11* gene, compared with patients with mutations in *RPS19* gene. (a) Representative immunoblots of erythroid precursors with RPS19 and RPL11 antibodies from DBA patients mutated in *RPS19* (left panel) and in *RPL11* (right panel) during terminal erythroid differentiation compared with controls. The expression levels were normalized with expression levels of actin. (b) Mean erythroid progenitor and precursor cell proliferation from peripheral CD34⁺ cells from controls ($n = 15$), DBA patients carrying mutations in *RPS19* ($n = 12$) or in *RPL11* ($n = 3$) gene from D0 to D12 during erythroid differentiation. Statistical test: Student's *t*-test

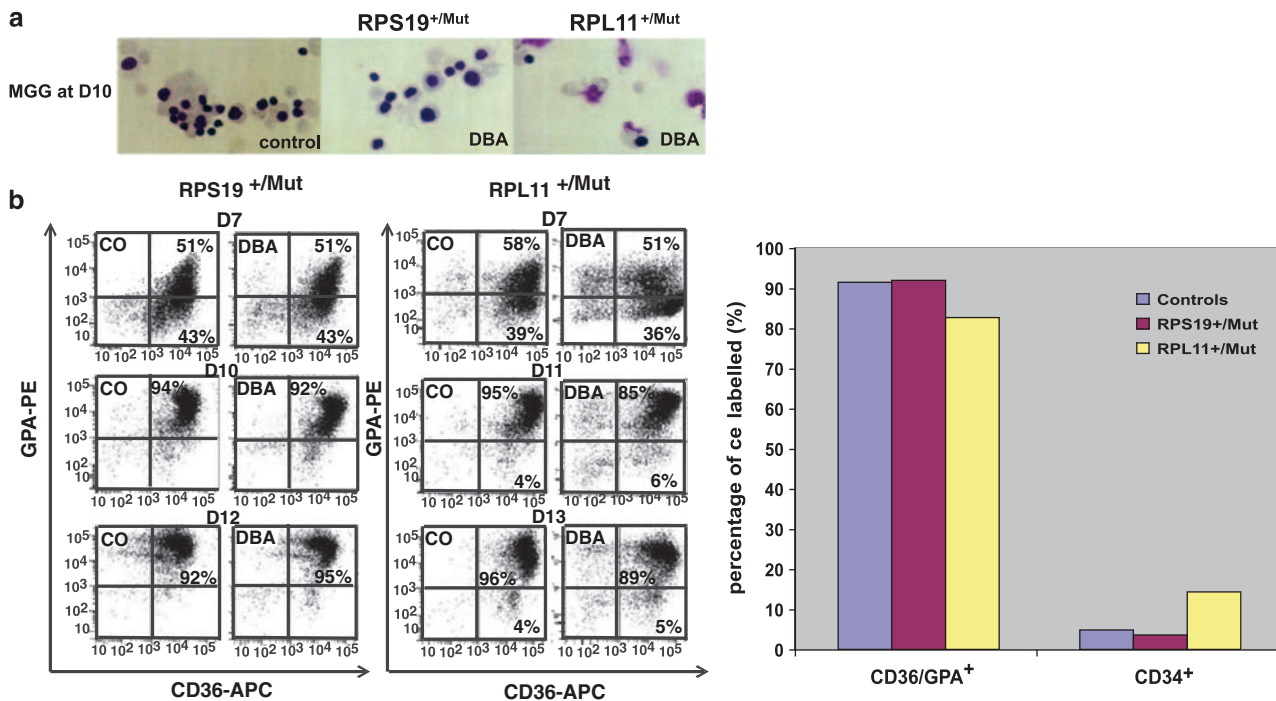


Figure 2 DBA patients with mutations in *RPS19* gene exhibited a normal erythroid differentiation phenotype compared with patients with mutation in *RPL11*, who exhibited a delay in erythroid differentiation. (a) May-Grünwald-Giemsa staining of the erythroid cells at D10 of terminal erythroid differentiation (orthochromatic erythroblasts) from controls, DBA patients with mutations in *RPS19* gene or in *RPL11* gene. The erythroblasts from the DBA patients with mutations in *RPS19* ($n = 12$) exhibited a normal terminal erythroid differentiation while the ones from the patients, who carry a mutation in *RPL11* ($n = 3$) exhibited a defect of terminal erythroid differentiation with a large number of necrotic cells. (b) Left panel: percentage of erythroid precursors (50 000 cells) labeled with the GPA/CD36 antibodies at D7, D10 and D12 of the terminal erythroid differentiation in DBA patients, one mutated in *RPS19*, one mutated in *RPL11*. Right panel: percentage of GPA/CD36⁺, CD34⁺ at D10 in the DBA patients carrying either a mutation in *RPS19* ($n = 2$) or *RPL11* ($n = 3$) gene compared with controls ($n = 8$). Cells from patients who carried a mutation in *RPS19* exhibited the same number of GPA/CD36⁺ or CD34⁺ cells as the controls. By contrast, erythroid precursors from patients, who carry a mutation in *RPL11* gene, exhibited a decrease in GPA/CD36⁺ cells and a large increase in CD34⁺ cells, suggesting a delay in erythroid differentiation

(Figure 2a). Accordingly, a slight decrease in the percentage of maturing cells (CD36⁺/GPA⁺ (glycophorin A)) was observed in cultures of RPL11-mutated cells ($n = 3$) compared with RPL19-mutated ($n = 2$) and control ($n = 8$) cells (Figure 2b), and the percentage of CD34⁺ erythroid cells was higher in RPL11-mutated cell cultures (Figure 2c). In addition, the percentage of apoptotic cells was much higher in RPL11-mutated cell cultures, as assessed by the quantitation of DAPI⁻/Annexin-V⁺ cells (Figure 3a), by the

TUNEL assay (data not shown), and by documentation of increased level of cleaved caspase-3 (Figure 3b).

Knockdown of RPS19 and RPL11 reduces the proliferation of erythroid precursors. As we are unable to obtain enough primary CD34⁺ cells from DBA patients to perform all the necessary studies, we used primary normal human CD34⁺ cells and shRNA-encoding lentiviruses to specifically inhibit RPL11 and RPS19 mRNA (Supplementary

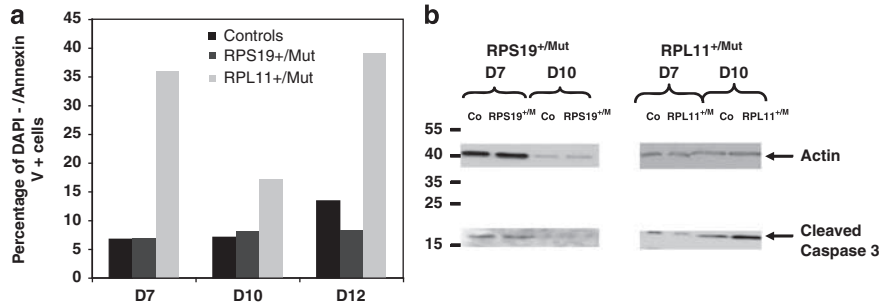


Figure 3 Degree of apoptosis in the DBA patients during erythroid differentiation. **(a)** Percentage of Annexin-V-positive cells during terminal erythroid differentiation in DBA patients, who carried mutation in *RPS19* (*RPS19*^{+/Mut}) ($n=2$) (dark grey plot), in *RPL11* (*RPL11*^{+/Mut}) ($n=3$) (light grey plot) compared with the controls ($n=8$) (black plot). The differences were statistically significant between controls and *RPS11*^{+/Mut} at days 7, 10 and 12 ($P<0.001$). Only two *RPS19*^{+/Mut} samples were studied for Annexin-V and statistical significance was not studied. However, nine other samples were studied by the TUNEL assay. If we pool the results from these two techniques investigating apoptosis, a much less statistical difference has been observed between controls and the *RPS19*^{+/Mut} samples ($P<0.05$) than for *RPS11*^{+/Mut}. **(b)** Representative western blot of cleaved caspase 3, protein involved in apoptotic pathway during terminal erythroid differentiation in one *RPS19*- and one *RPL11*-mutated DBA patients compared with their controls

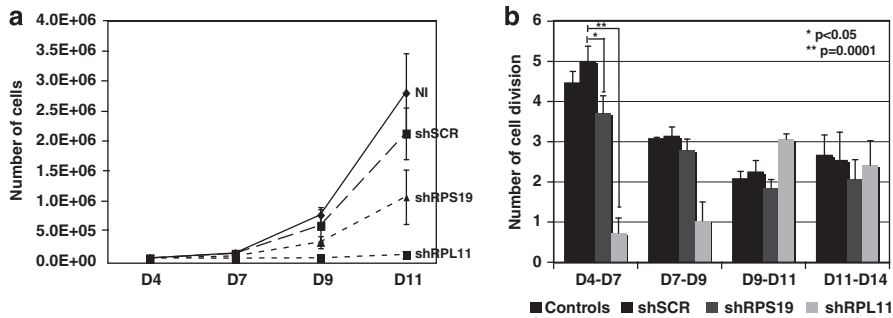


Figure 4 Depletion of *RPS19* or *RPL11* induces a decrease in cell growth. **(a)** Cell growth curves during erythroid differentiation following infection with *shRPS19* and *shRPL11* compared with the non-infected cells or infected with the *shSCR* (three independent experiments). **(b)** Number of cell divisions calculated at several time points according to the formula: number of cell division = $\log(\text{extent of amplification})/\log 2$. Data from three independent experiments

File 1A–C). The efficacy of shRNA was validated in UT-7 cells and in 7-day erythroid cultures of cord blood CD34⁺ cells. One of the three shRNAs targeting *RPL11* tested, *shRPL11A* induced a 95% and a 65% decrease in *RPL11* mRNA level in UT-7 and erythroid cells, respectively, whereas a previously described *shRPS19C*²⁵ induced a 90% and a 50–70% decrease in *RPL19* mRNA level in UT-7 and erythroid cells, respectively (Supplementary File 1B). At the protein level (Supplementary File 1C), the decrease obtained in *RPS19* protein expression (40–55%) was consistently lower than that noted for *RPL11* expression (decrease of 60–90%), which mimicked the situation observed in primary cells from DBA patients (Figure 1a). Proliferation of erythroid cells following depletion of *RPS19* and *RPL11* was assayed by counting cells in triplicate at various times following initiation of cell culture in four independent experiments. Although no difference in proliferation was noted between non-infected cells and cells infected with the irrelevant shRNA (*shSCRamble*), *shRPS19* induced a decrease in cell proliferation (Figure 4a and Supplementary File 2) an effect that was even more pronounced following infection with *shRPL11* (Figure 4a and Supplementary File 2). As shown in Figure 4b and Supplementary File 2, the largest decrease in cell proliferation was noted between D4 and D7.

Depletion of *RPL11* specifically delays erythroid differentiation with increased apoptosis. Flow cytometry using the differentiation antigens CD34, CD36, CD71 and GPA showed a delay in erythroid differentiation following *RPL11* depletion but not following *RPS19* depletion. Indeed, the same percentages of CD36⁺/GPA⁺ cells (50 ± 9%) and CD71⁺ (79 ± 6%) were present after *shRPS19* treatment as in controls (42 ± 9% and 53 ± 13% of CD36⁺/GPA⁺, 78 ± 1% and 85 ± 4% of CD71⁺ in non-infected and *shSCR*-infected cells, respectively; Figures 5a and b). In contrast, less CD36⁺/GPA⁺ (20 ± 9%) and CD71⁺ (31 ± 15%) cells were found following infection with *shRPL11* (Figures 5a and b). This was related to a blockage or delay in erythroid differentiation as more residual CD34⁺-positive cells were detected in *RPL11* (24 ± 10%)-depleted cell cultures than in control (8 ± 1% and 4 ± 1.5%) and *RPS19* (7 ± 3%)-depleted cell cultures (Figure 5b).

Cytological examination showed that *RPL11*-depletion induced the appearance of apoptotic cells at day 7, which was not seen in controls and *RPS19*-depleted cells (data not shown). Flow cytometry analyses confirmed that *RPL11* depletion induced a striking increase in the percentage of Annexin-V-positive cells at D7 (Figure 5c), and immunoblot experiments detected cleaved caspase-3 and cleaved poly (ADP-ribose) polymerase (PARP) in *RPL11*-depleted cells,

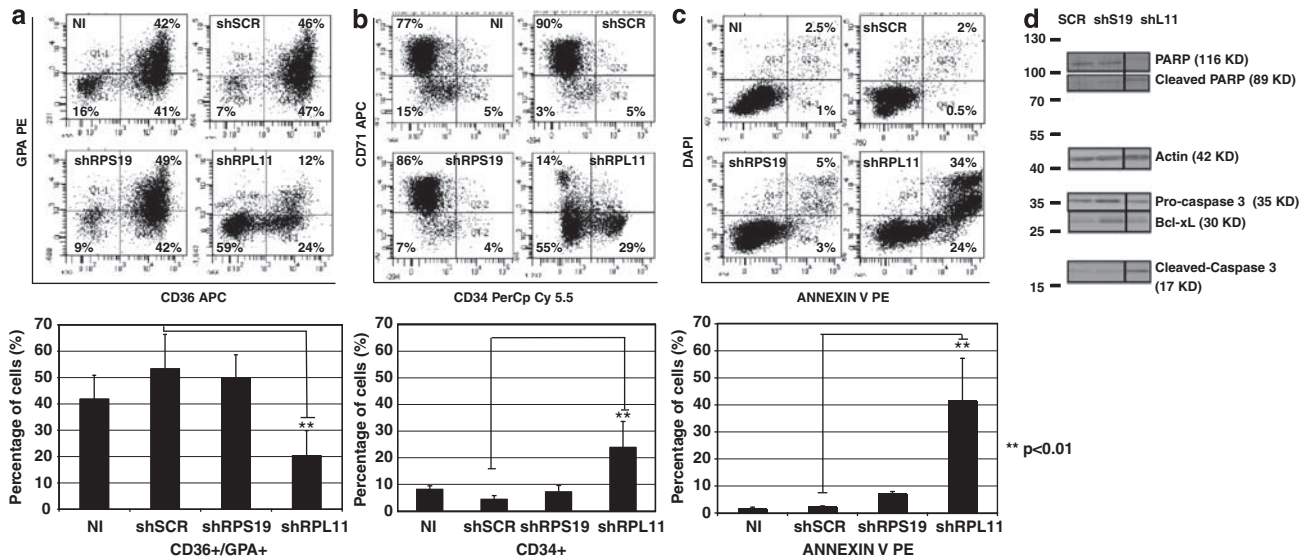


Figure 5 Delayed erythroid differentiation following depletion of RPL11. (a) Decreased numbers of CD36⁺/GPA⁺ cells following infection with shRPL11 compared with shRPS19-infected and various control cells (three independent experiments). (b) Less CD71⁺ cells and more immature CD34⁺ cells following infection with shRPL11 compared with shRPS19-infected and various control cells (three independent experiments). (c) Top and bottom panels: increased apoptosis following depletion of RPL11, with more Annexin-V-positive cells in cells infected with shRPL11 compare with RPS19 depletion (three independent experiments). (d) Expression level of the major proteins involved in apoptosis (caspase 3 and cleaved caspase 3, PARP and cleaved PARP) or anti-apoptotic protein such as Bcl-X_L following infection of cord blood CD34⁺ with specific shRPS19 or shRPL11 compared with the shSCR infection

which was not observed in controls and in RPS19-depleted cells, in which Bcl-X_L was increased (Figure 5d). These findings are consistent with the higher degree of apoptosis observed in primary CD34⁺ cells with reduced expression of RPL11 due to gene mutations.

p53 pathway is activated in primary CD34⁺ cells from DBA patients and following RPS19 or RPL11 depletion in normal CD34⁺ cells.

We analyzed the p53 pathway in erythroid cells from six DBA patients – three with mutant RPS19 (RPS19^{+mut}) and three with mutant RPL11 (RPL11^{+mut}). Increased level of p53 was noted in all DBA patients, suggesting stabilization of the protein (Figures 6a and b). Furthermore, the transcript of p21, a primary target of p53, was markedly increased in erythroid cells with mutant RPS19 (32.3-fold, and 7.4-fold at D7 and D10, respectively) and with mutant RPL11 (17-fold and 49.4-fold at D7 and D10, respectively) confirming activation of p53 (Figure 6a). An increase in p53 and phospho-p53 protein expression levels was also observed in the DBA patients and in RPS19- and RPL11-depleted CD34⁺ cells (Figures 6b and d, Supplementary File 3), with RPL11 depletion increasing the protein levels to a higher extent than RPS19 depletion. To further confirm the activation of p53, we tested the transcript levels of three p53 targets (p21, Bax and Noxa). Following depletion of RPL11, significant increase in transcripts of all three targets was noted with the most notable increase (16.2-fold) seen for p21. The effect of RPS19 depletion was less pronounced with a slight increase in Bax (twofold) and a larger increase in p21 (fivefold), with no increase in Noxa mRNA (Figure 6c). Although an increase in p21 protein was observed with both RPS19 and RPL11 shRNAs, the increase in Bax protein expression level was most pronounced

following depletion of RPL11 (Figure 6d). Taken together, these results show that depletion of RPS19 and that of RPL11 lead to differential activation of the p53 pathway in erythroid cells.

As the documented decrease in cell proliferation cannot be totally explained by apoptosis, especially after RPS19 depletion, we studied cell cycle progression of erythroid cells derived from primary CD34⁺ cells of two RPL11^{+mut} DBA patients and following RPS19 and RPL11 depletion in normal CD34⁺ cells (Figure 7). An increased number of cells in G₀/G₁ phase was observed in both patients carrying RPL11 mutation, which was more significant at D13 than at D10 (Figure 7a). A small increase in cells in G₀/G₁ phase was also noted following infection with the shRPS19 (49 ± 0.6%) compared with either non-infected cells (43 ± 0.6%) or cells infected with shSCR (42 ± 0.4%) (Figure 7b top and bottom panels). Depletion of RPL11 induced a slightly larger increase in the number of cells in G₀/G₁ phase (59 ± 0.5%). In parallel, a decrease in percentage of cells in S and in G₂/M phases was noted (Figure 7b). Moreover, cells in subG₁, which represent apoptotic cells, were present following infection with shRPL11 (8 ± 0.8%), confirming that increased apoptosis is a feature of RPL11 depletion (Figure 7b).

p53 activation is responsible for apoptosis and the G₀/G₁ cell cycle arrest.

To further define the role of p53 activation, we performed a dual shRNA infection, first with either green fluorescent protein (GFP)-shRPS19 or GFP-shRPL11 on day 1, then by a Cherry-shp53 infection on day 2. The efficiency of the shp53 was confirmed in UT7 and CD34⁺ cells by documenting decreases in p53 mRNA and in protein expression levels (Figure 8a). Following decreased expression of p53, proliferation of both

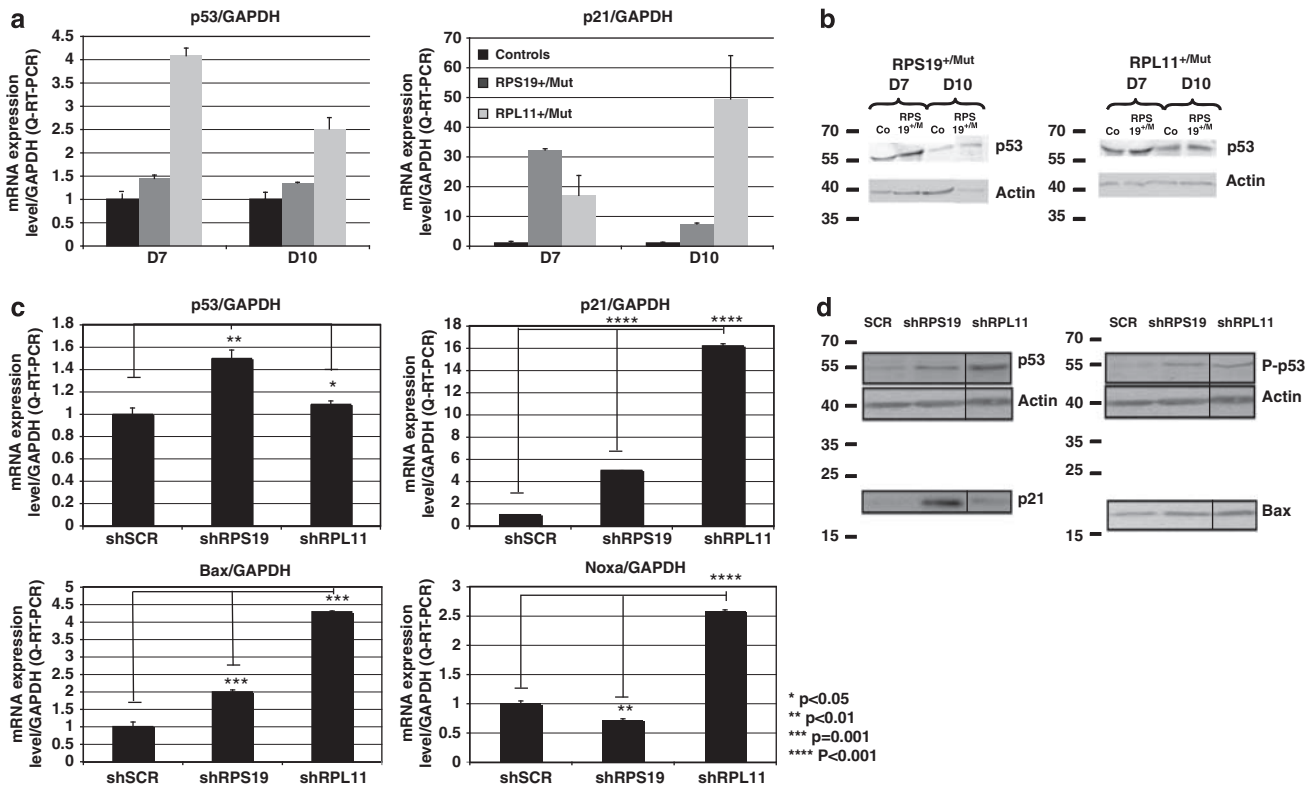


Figure 6 p53 activation in DBA patients carrying mutations in *RPS19* or in *RPL11* gene or after CD34⁺ cell infection with shRPS19 or shRPL11. (a) p53 mRNA and p21 mRNA expression level by quantitative RT-PCR (ratio to GAPDH mRNA level) in DBA patients carrying mutation in *RPS19* (dark gray plot) or *RPL11* (light gray plot) genes compared with the controls (black plot) at day 7 and day 10 during erythroid differentiation. (b) Western blot analyses of p53 in two patients who carried, respectively, a mutation in *RPS19* and in *RPL11* gene at D7 and D10 compared with controls. (c) mRNA expression level of p53, p21, Bax and Noxa compared with GAPDH mRNA by quantitative-RT-PCR at day 7 of the erythroid differentiation after cord blood CD34⁺ infection with the shRPS19 or shRPL11 compared with shScramble infection (three independent experiments). (d) Protein expression levels of p53, phosphorylated p53, and p21 and Bax determined by western blot analysis following infection with shRSP19 or shRPL11 compared with the Scramble at day 7 of the erythroid differentiation (representative of three independent experiments)

RPS19- and *RPL11*-depleted erythroid precursors increased after day 9 (Figure 8b). Strikingly, we were also able to inhibit the activation of apoptosis induced by *RPL11* depletion (Figure 8c). p53 mRNA level returned to normal after p53 depletion in *RPS19*- and *RPL11*-depleted cells (Figure 8d). Increased expression levels of p21, Bax and Noxa mRNA noted following infection of CD34⁺ cells with either shRPL11 or shRPS19 was significantly reduced following p53 knock-down (Figure 8d). These results confirm that the erythroid phenotypes due to *RPS19* and *RPL11* depletion depend on p53 activation. Of particular interest, the finding that there is no increase in *RPL11* expression levels following depletion of either *RPS19* or *RPL11*, implies that increased levels of *RPL11* is not necessary for p53 activation pathway (Figure 8e).

Discussion

In spite of the significant progress made in identifying mutations in ribosomal genes *RPS19* and *RPL11* in $\approx 30\%$ of DBA patients, the mechanistic understanding of how these mutations account for DBA pathogenesis including erythroblastopenia remains to be fully defined. Erythroblastopenia in DBA is the result of an intrinsic defect with blockade in erythroid differentiation that occurs just following the BFU-e/

CFU-e (burst-forming unit erythroid/colony-forming unit erythroid) transition or between erythropoietin (EPO)-independent and EPO-dependent stages.²⁶ To identify the link between depletion of a RP and the erythroblastopenia in DBA-affected individuals, we investigated proliferation and differentiation of primary hematopoietic cells obtained from DBA patients in the French DBA registry. We obtained two distinct phenotypes, decreased proliferation with either no apoptosis or increased apoptosis, *in vitro* depending on the RP mutated. Primary cells from patients harboring mutations in *RPS19* gene or normal cells following depletion of *RPS19* by specific shRNA exhibited decreased proliferation of erythroid cells. However, there was neither alteration of the terminal erythroid differentiation as already reported in *RPS19*-deficient TF1 cell lines²⁷ nor significantly increased apoptosis. In marked contrast, in patients with *RPL11* mutation or following *RPL11* depletion by specific shRNA, we identified a more pronounced phenotype: a greater extent of decrease in cell proliferation, delayed erythroid differentiation and marked increase in apoptosis. The fact that we recapitulated exactly the same phenotypes in primary cells from patients harboring the RP mutations and in normal cells following RP depletion reflects true differential effects of different RPs on erythroid differentiation.

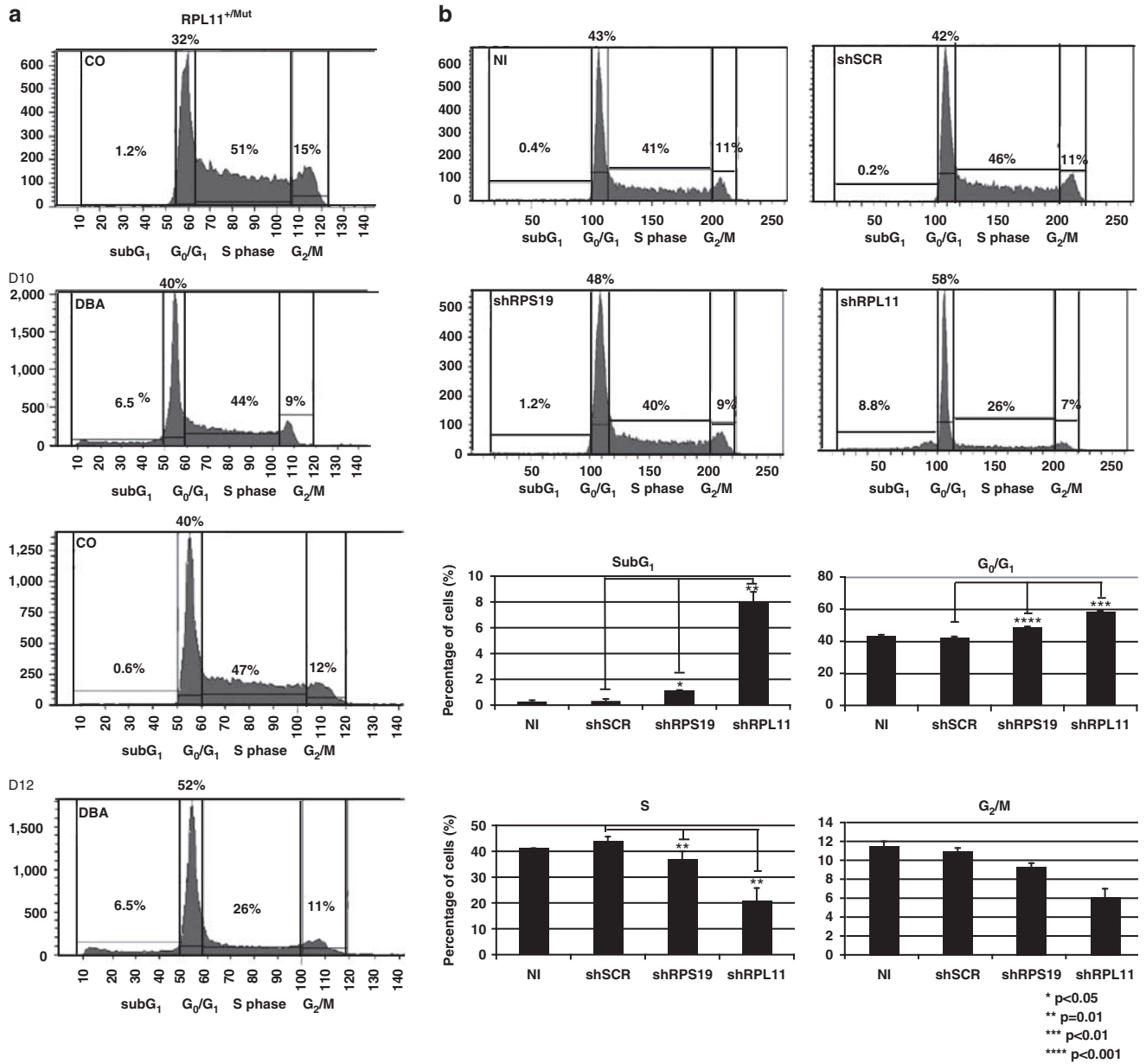


Figure 7 Depletion of RPS19 and RPL11 induces cell cycle arrest in G₀/G₁ phase. (a) Cell cycle analysis of erythroid cells from a patient carrying mutation in *RPL11* during erythroid differentiation. Cell cycle arrest in G₀/G₁ phase with an increased percentage of cells in subG₁ phase, corresponding to apoptotic cells can be seen. (b) Representative histograms from cell cycle analysis following depletion of RPS19 and RPL11 by specific shRNA. Percentages of cells in various phases of cell cycle: G₀/G₁, S, G₂M. Following infection with the shRPS19, there is an increased number of cells blocked in G₀/G₁ phase compared with the controls. Depletion in RPL11 induced an even larger increase in cells blocked in G₀/G₁ phase with an accumulation of cells in subG₁ phase, which reflects increased numbers of apoptotic cells (three independent experiments)

Earlier studies using model organisms have implicated a role for p53 pathway in DBA pathogenesis. In a Dark skin (*Dsk3*^{+/-}) mouse model with a RPS19 missense mutation²¹ and in a morpholino-induced RPS19-deficiency in zebrafish,^{19,23} elevated expression levels of p53 were found to account for the observed phenotype, which included growth retardation, a delay in erythroid differentiation and congenital abnormalities that mimic some DBA phenotypes in humans. The zebrafish morpholino RPL11¹⁸ also induced p53 activation and developmental abnormalities. The present study was

performed in primary cells from a large cohort of 15 DBA patients in which we document p53 activation and cell accumulation in G₀/G₁ in all the DBA patients analyzed and in normal cells depleted from RPS19 or RPL11. The extent of p53 activation was consistently higher in RPL11-depleted cells compared with RPS19-depleted cells. We validated that the observed decrease in cell proliferation and increase in apoptosis are directly related to p53 activation by showing that both these defects could be reversed by RNA interference-mediated p53 knockdown.

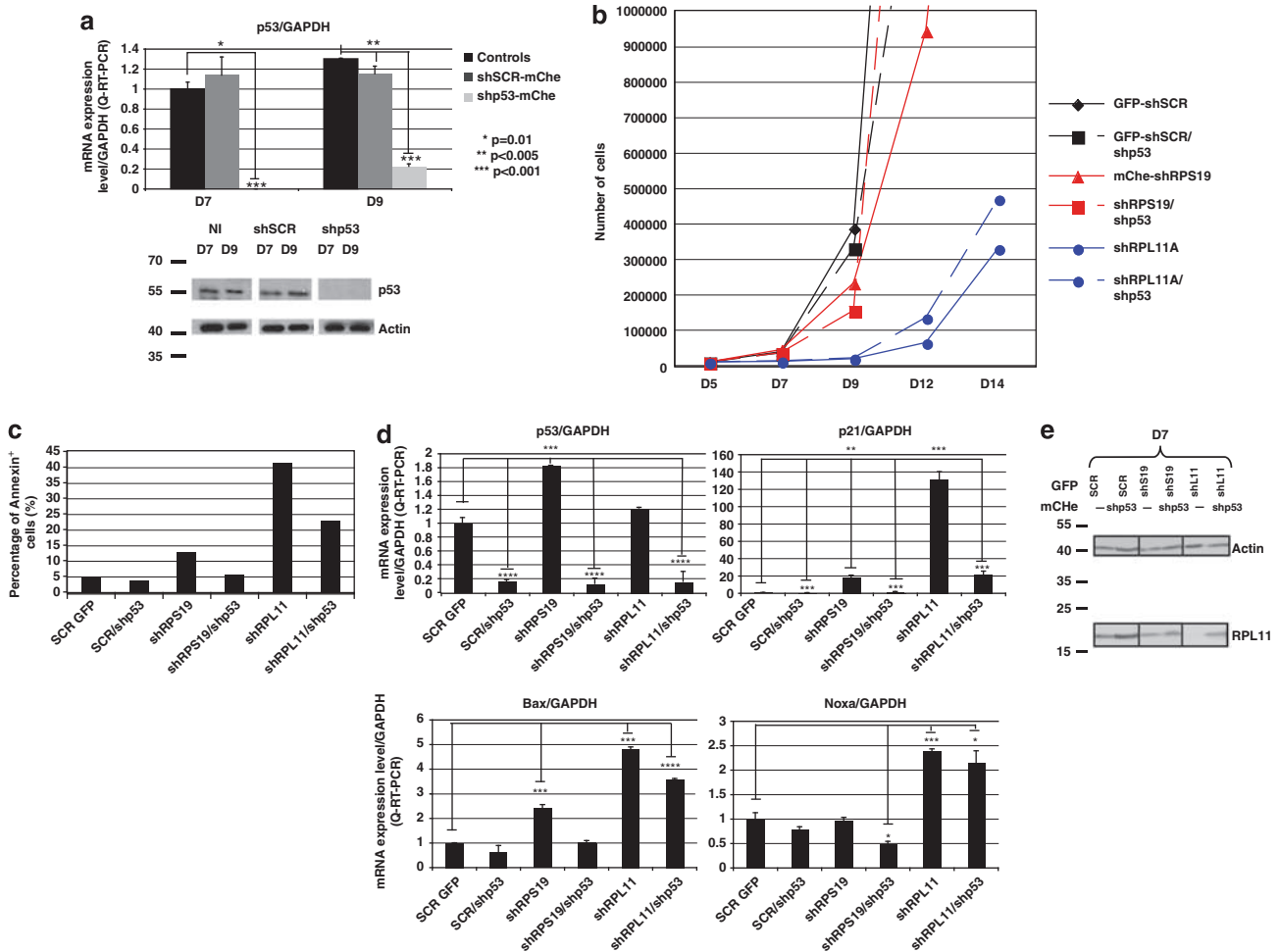


Figure 8 p53 inhibition reversed the erythroid proliferation blockade after RPS19 depletion in CD34⁺ cells and both the erythroid proliferation blockade and apoptosis activation after RPL11 depletion. **(a)** Efficiency of the shp53 CD34⁺ cells: Left panel, the mCherryshp53 is able to reduce completely the level of p53 mRNA at day 7 and to 20% at day 9 compared with the p53 mRNA level in non-infected cells (NI) or infected cells with the shSCR-mCherry; right panel: decreased p53 protein expression level at day 7 and 9 after CD34⁺ infection with the shp53-mCherry compared with the shSCR-mCherry and non-infected cells (NI; three independent experiments). **(b)** The erythroid proliferation blockade in DBA is dependent on p53 activation in RPS19 and RPL11-depleted erythroid precursor cells: Erythroid progenitor and precursor cell amplification curve from day 0 to day 14 from CD34⁺ infected with the shSCR-GFP (full black line), or with the shSCRGFP-shp53mCherry (interrupted black line), or with the shRPS19GFP alone (full red line) or after a coinfection shRPS19GFP and shp53mCherry (interrupted red line) or with the shRPL11GFP alone (full blue line) or after a coinfection shRPL11GFP and shp53mCherry (interrupted blue line). **(c)** Activation of the apoptosis is also dependent on p53 activation in RPL11 depleted erythroid precursor cells: Percentage of DAPI⁻/Annexin-V⁺ cells at day 7 by flow cytometry in CD34⁺ cells infected CD34⁺ infected with the shSCR-GFP, or with the shSCRGFP-shp53mCherry, or with the shRPS19GFP alone or after a coinfection shRPS19GFP and shp53mCherry or with the shRPL11GFP alone or after a coinfection shRPL11GFP and shp53mCherry. Knockdown of p53 decrease to the amount of apoptotic cells after RPL11 depletion by half. **(d)** The activation of p21, Bax and Noxa is dependent on p53 activation: The mRNA level of p53, p21, Bax and Noxa measured at day 7 during erythroid differentiation by quantitative RT-PCR compared with the GAPDH reporter gene decreased significantly after coinfection of the depleted RPS19 or RPL11 cells with the shp53m-Cherry (three independent experiments) **P* < 0.05, ***P* < 0.01, ****P* < 0.005, *****P* < 0.0001. **(e)** RPL11 increased expression level is not necessary for p53 activation in RPS19 and RPL11 depleted cells. Western blot analyses of the protein expression level of RPL11 after CD34⁺ infection with the shRPS19 or the shRPL11 compared with actin protein level. RPL11 protein was not increased in RPS19-depleted cells compared with the controls (shSCR) and as expected decreased after depletion of RPL11 by the shRPL11. Knockdown of p53 in depleted RPS19 or RPL11 erythroid cells increased the protein expression level of RPL11 but to a less extent as the control (shSCRGFP/shp53)

Our findings with primary human DBA cells validate the findings from murine and zebrafish models that p53 has a key role in the decreased erythroid proliferation in DBA pathophysiology. Kuramitsu *et al.*²⁸ have previously shown that decreased expression of RPS19 in CD34⁺ cells induces cell cycle arrest with an accumulation of cell in G₀ and no apoptosis, findings consistent with data from the present study. More recently, Badhai *et al.*²⁹ showed that RPS19 insufficiency in primary fibroblasts of DBA patients causes cell

cycle arrest in G₁ phase, which correlated with marked decreases in CDK2, cyclin D and phosphorylated pRB, indicating an impaired progression into S phase. Interestingly, this phenotype was associated with a normal level of p53 in primary fibroblasts of DBA patients, probably because fibroblasts are less sensitive to stress induced by mutations in *RP* genes. Our results are also in agreement with those of Dutt *et al.*,³⁰ who observed cell cycle arrest and an activation of p53 pathway following depletion of RPS19. The activation

of p53 pathway due to mutations in RPS19 may be mediated by nucleolar stress due to a defect in rRNA maturation such as that identified in the 3'UTR of the ITS1 at the A2 cleavage site of the 18S rRNA.^{13,15,16} It is well established that a rRNA maturation defect generates nucleolar stress or ribosomal stress. After ribosomal stress, levels of RPL5, RPL11,^{31–33} RPL23,³⁴ RPS3³⁵ and RPS7³⁶ are increased in the nucleoplasm, which in turn sequester MDM-2 (or human double minute 2 (HDM-2) in human) and prevent it from binding to p53, its natural inhibitor. MDM-2 (or HDM-2), an E3 ubiquitin ligase, has a role in ubiquitinating p53 and its resultant degradation by the proteasome. In the event of a ribosomal stress, MDM-2 (or HDM-2) fails to bind p53, and as a result, p53 is not ubiquitinated and thus not degraded by the proteasome.^{31–36} In addition, Fumagalli *et al.*²⁴ have shown that, without nucleolar stress in hepatocytes, haploinsufficiency in RPS6, RPS23 and RPL7a leads to an upregulation of RPL11. Recently, Dutt *et al.*,³⁰ has shown that RPS14 or RPS19 depletion after CD34⁺ infection with specific shRNAs leads to p53 activation without nucleolar disruption but through HDM-2 binding to RPL11. In DBA patient CD34⁺ cells, it is too speculative at this time to define how a mutation in a *RP* gene leads to an activation of p53 and if HDM-2 is involved but our future studies will focus on deciphering these mechanisms. However, we were able to show that p53 is activated in RPL11-mutated DBA patients and in native CD34⁺ cells infected by shRPL11, which in both cases led to a large decrease in RPL11 protein expression level. As such, it appears that p53 can be activated without increased RPL11 expression level. There is preliminary evidence that p53 may be activated by different mechanisms during a ribosomal stress, one through the RPL11-HDM2-p53 pathway and the other through p38 activation. It is thus possible that p53 activation mechanism(s) following RPS19 or RPL11 depletion may not be the same, which may account for the observed differences in the extents of p53 activation.

In summary, our findings imply that deficiencies in RPS19 and RPL11 activate p53 to different extents, leading to differential effects on erythropoiesis. Furthermore, our findings have enabled us to establish that increased level of RPL11 expression is not necessary to activate p53 in erythroid cells. An unanswered question is whether the entire erythroid phenotype of DBA is related to increased expression levels of p53 or if additional p53-independent mechanisms may also have a role in the pathogenesis of the disease.

Materials and Methods

Population. A total of 15 unrelated patients affected with DBA and 15 hematologically normal individuals were studied. The DBA patients are registered in the French DBA registry. DBA was diagnosed according to the established criteria.¹ All cases were reviewed in detail at the time of analysis, and Table 1 shows the biological and clinical data of the 15 DBA patients, which have been obtained from the institutions and physicians responsible for the patient's management. Informed consent was obtained in accordance with the Declaration of Helsinki. Human umbilical cord blood was collected from normal full-term deliveries after maternal informed consent was approved according to institutional guidelines (AP-HP, Paris, France).

Lentiviral vector construction, production and cell infection.

shRNA cloning. The RPS19 shRNA used in the present study was previously described by Flygare.²⁵ Three different shRNA sequences against RPL11 were

synthesized (Eurogentec, Angers, France) and cloned into a pBlue Script containing the human *H1* promoter (Généthon, Evry, France). The H1-shRPS19C, H1-shRPL11A, -L11B, -L11C and H1-SCR (scramble control sequence) cassettes were cloned into a lentiviral vector, pRRLsin-PGK-eGFP-WPRE (Généthon; Supplementary File 1A). The sequence of the various cloned fragments was confirmed by cDNA sequencing. Oligonucleo-hairpins sequences of RPS19 and RPL11 short hairpins (shRNAs) used in the present study are available upon request. The p53 shRNA sequence was described Brummelkamp *et al.*³⁷ We modified the pRRLsin-PGK-eGFP-WPRE including a Cherry sequence instead of eGFP to collect by cell sorting the positive cells for both GFP (shRPS19- and shRPL11-infected cells) and cherry (shp53-infected cells). pm-Cherry C1 plasmid (Clontech, Saint-Germain-en-Laye, France) was digested by *SgrAI/XmaI* then religated. The modified Cherry cassette was amplified by PCR introducing *Sall/BamHI* restriction sites and used as replacement of the *Sall/BamHI* GFP cassette of pRRL-PGK GFP. Blunt vector from a *XhoI/EcoRI* digest of SuperRetro-pH1-shp53-PGK-Puro were ligated using standard ligation protocol.

Lentiviral production. Lentiviral stocks were prepared as previously described³⁸ and stored at -80°C . Titers of viral particles were determined by quantifying the number of GFP or mCherry-positive cells following infection of HEK 293 T cell lines.

Cell infection and culturing of UT-7 cells. UT-7 cells were infected at day 1 at multiplicity of infection (MOI) of 10 in Iscove's 4 modified Dulbecco's media (IMDM; Invitrogen, Cergy-Pontoise, France), 10% of fetal bovine serum (FBS) and 5 ng/ml granulocyte macrophage colony-stimulating factor. GFP- or mCherry-positive cells were sorted 2 days later using a FACSVantage Cell Sorter (Becton Dickinson Biosciences, Le Pont de Claix, France). The effectiveness of shRNA in downregulating specific mRNA and the protein was assessed 2 days following isolation of sorted cells (Supplementary File 1B and C).

Erythroid cell proliferation and differentiation of CD34⁺ cells, apoptosis and cell cycle analysis. CD34⁺ cells from peripheral blood of DBA patients and control subjects or cord blood were isolated by the immunomagnetic technique (Miltenyi Biotec, Paris, France). Purified CD34⁺ cells from DBA patients and controls were cultured in IMDM medium (Invitrogen) containing 1% L-glutamine (Invitrogen), 1% penicillin-streptomycin (Invitrogen), α -monothio glycerol (Sigma-Aldrich, Lyon, France), 1.5% bovine serum albumin (Stemcell Technologies, Sheffield, UK), iron-saturated transferrin (Sigma-Aldrich) and 2% liposomes, 50 ng/ml stem cell factor (SCF), 1 U/ml interleukin-3 (IL-3), 1 U/ml EPO and 10% FBS. At day 7, cultures were switched to the same medium but with 30% FBS (from D7 to D12). For some DBA patients, we performed *in vitro* erythroid cultures in two phases: a first phase of 7 days in methylcellulose with EPO (3 U/ml), SCF (50 ng/ml) and IL-3 (30 U/ml) and a second phase in liquid culture.

For lentiviral infection, CD34⁺ cells were cultured for 2 days in the presence of 10% FBS, 100 U/ml IL-3, 10 ng/ml IL-6, 25 ng/ml SCF, 10 ng/ml thrombopoietin and 10 ng/ml Flt3-L (Fms-related tyrosine kinase 3-ligand). A first infection was then performed at a 50 MOI. In the case of shRNA-RPS19C, a second infection was performed 6 h after the first infection (Supplementary File 2). Cells were cultured for 2 more days and GFP-positive cells were sorted using the FACSDIVA Cell Sorter. Sorted cells were switched to the same IMDM medium with SCF (50 ng/ml), IL-3 (1 U/ml) and EPO at 1 U/ml till D7 when the FBS concentration was increased to 30% (from D7 to D14).

Viable cells were counted using the trypan blue dye exclusion test as a function of time in culture. Following May-Grünwald-Giemsa staining, extent of terminal erythroid differentiation was evaluated by morphological assessment.

Erythroid differentiation was also evaluated by flow cytometry (FACS Canto, Becton Dickinson Biosciences). Cells were immunophenotyped from D7 to D14 using several antibodies: phycoerythrin (PE)-coupled anti-GPA (Caltag, Burlingame, CA, USA), allophycocyanin (APC)-conjugated anti-CD36, PerCP-cy5.5-conjugated anti-CD34, APC-anti-CD71 (Becton Dickinson Biosciences) and PC7-conjugated anti-CD34 (Beckman Coulter, Villepinte, France). Isotype controls were obtained from Becton Dickinson Biosciences.

For determining apoptosis, cells were stained with PE-conjugated Annexin-V (Becton Dickinson Biosciences) and with DAPI (Sigma-Aldrich, Saint-Quentin-Fallavier, France) according to the manufacturer's protocol. In addition, in DBA patients, the TUNEL method was performed according to the manufacturer's

protocol (kit ApopDETEK, DAKOCytomation, Enzo Diagnostics Inc., Farmingdale, NY, USA) on the cells isolated from erythroid colonies and the percentage of apoptotic cells was determined based on microscopic counting of 200 cells. Cell cycle was studied at day 7, 10 and D12 following propidium iodide staining (Sigma-Aldrich) by flow cytometry.

Real-time quantitative RT-PCR.

RNA extraction. Total RNA was extracted using TRIzol reagent (Invitrogen) and treated with RNase-free DNase (Qiagen, Courtabouef, France). The quality of the RNA was verified on an agarose gel and quantified with a Nanodrop spectrophotometer (ND-1000 UV-Vis; Thermo Scientific, Wilmington, DE, USA).

Reverse transcription-PCR. cDNA was synthesized from extracted RNA with SuperScript II RNase H-Reverse transcriptase kit (Invitrogen).

Real-time quantitative RT-PCR. Primers and internal probes for quantitative reverse-transcriptase (QRT)-PCR were designed using Primer Express Software (Perkin-Elmer Applied Biosystems, Foster city, CA, USA) and are available upon request. PCR was carried out in the ABI Prism GeneAmp 5700 Sequence Detection System (Perkin-Elmer) using the TaqMan Universal PCR Master Mix (ABI) containing the specific primers (1.5 μ M) and specific probe (0.1 μ M). The expression level of each gene was normalized using three housekeeping genes – hypoxanthine-guanine-phosphoribosyl-transferase (*HPRT*) gene, glyceraldehyde-3-phosphate dehydrogenase (*GAPDH*) gene and β 2 microglobulin (β 2 *microglobulin*) gene.

Western blot analysis. Each pellet of 50 000 cells from the DBA patients and 125 000 cells from shRNA-infected CD34⁺ cells was lysed in Laemmli buffer (100 mM Tris pH 6.8, 10% glycerol, 4% SDS, 0.2% blue Bromophenol, 20 mM dithiothreitol), sonicated (five times, 15 s) in ice water and boiled for 5 min. Samples were run on a Tris glycine 10% SDS-PAGE resolving gel. Following electrophoresis, proteins were transferred onto a PVDF Hybond-P membrane (GE Healthcare Europe, Orsay, France) and stained with Ponceau S solution (Sigma-Aldrich, Lyon, France) to assess quantity of transferred proteins. Following washing of the membranes with Tris-buffered saline with 1% Tween-20 (TBST 1 \times), membranes were soaked in blocking buffer (4% milk, 1% bovine serum albumin, 0.2% sodium azide in TBST 1 \times) for 1 h and then immunolabeled overnight at 4 °C with the different antibodies. Antibodies used for immunoblots were as follows: p53, phospho p53 (ser15), caspase 3, cleaved caspase 3, Bcl-X_L, PARP antibodies (all rabbit polyclonal antibodies from Cell Signaling, Ozyme, Saint Quentin Yvelines, France); p21 (2947) (rabbit monoclonal, Cell Signaling, Danvers, MA, USA), Bax antibody (rabbit polyclonal, Abcam, Cambridge, MA, USA) and β -actin antibody (Ac-15; Sigma-Aldrich). The polyclonal chicken RPS19 antibody,³⁹ the monoclonal RPS19 mouse antibody kindly provided by F Loreni⁴⁰ or the commercial antibodies against RPS19 (monoclonal mouse SC100836, Santa Cruz Biotechnology, Inc. (Santa Cruz, CA, USA) and mouse monoclonal 57 643, Abcam), the antibody against RPL11 were used at the appropriate dilution. Following several washes with TBST 1 \times , membranes were incubated with appropriate secondary antibodies for 1 h. After several washes with TBST 1 \times , the membranes were soaked in ECL solution (GE Healthcare) and the expression level of various proteins determined on the Amersham hyperfilm ECL (GE Healthcare).

Statistical analysis. Data are presented as the mean \pm standard error of the mean (\pm S.E.M.) or standard deviation (S.D.). Student's *t*-test was used to compare the data from different populations.

Conflict of Interest

The authors declare no conflict of interest.

Acknowledgements. We are grateful to Professor Eric Solary (INSERM U1009, Villejuif, France) for scientific discussions. We thank Dr. F Loreni for providing us the monoclonal mouse antibody against RPS19 (Department of Biology, University 'Tor Vergata', Roma, Italia). We thank Dr. Stefan Constantinescu (Ludwig Institute for Cancer Research, Brussels, Belgium) and Dr. Guido Bommer (Duke Institute and Université catholique de Louvain, Brussels, Belgium) for providing us the SuperRetro-pH1-shp53-PGK-Puro construction. We thank Drs

E Lainey and O Fenneteau (Hematology Laboratory, Robert Debré Hospital, Paris, France) for their advice on cytology and cytometry; Maud Simansour, Claudia Spangenberg (Hematology Laboratory, Robert Debré Hospital, Paris, France) and Alexis Proust (Hôpital Bicêtre) for the mutation screening analysis of DBA patients; Isabelle Marie for managing the French DBA registry; and Patricia Rincé for the help in the methylcellulose culture (both from Hôpital Bicêtre, Le Kremlin-Bicêtre, France). We deeply appreciate the cooperation of DBA patients and their families, all the physicians involved in the patient care and management, who provided us the clinical and biological data and some blood samples. We thank the French DBA patient's association (AFMBD), the DBA Foundation and Daniella Maria Arturi Foundation for their support. This work was supported by the Institut National de la Santé et de la Recherche Médicale (INSERM), France; NIH Grants HL079565 and DK32094, USA; l'Agence Nationale de la Recherche (ANR RIBODBA and ANR RIBOCrash), France; la Fondation pour la Recherche Médicale (FRM) France; l'Association pour la Recherche sur le Cancer (ARC), France; the DBA Foundation and the Daniella Maria Arturi Foundation, USA.

Author Contributions

Hélène Moniz performed the vast majority of experiments and analyzed the data. Marc Gastou performed most of the experiments with the shp53. Thierry Leblanc provided us the DBA patient data and samples. Corinne Hurtaud helped in the purification of CD34⁺ cells and performing erythroid cell cultures. Aurore Crétien performed methylcellulose cultures of CD34⁺ cells and analyzed erythroid differentiation from the DBA patients. Marlène Flaubladier produced and provided us the antibody against RPL11. Laure Croisille performed the clonogenicity assays. Yann Lécluse performed the sorting of the GFP-positive cells by flow cytometry. Jérôme Larghero provided cord blood samples. Hanna Raslova helped us with the design of the lentiviruses. Olivier Bluteau and Larissa Lordier generated the mCherry-shp53. Gil Tchernia and William Vainchenker provided clinical and scientific insights. Narla Mohandas participated in study design and wrote the article with Lydie Da Costa and Hélène Moniz. Lydie Da Costa designed the studies, analyzed the data and directed the research project.

- Vlachos A, Ball S, Dahl N, Alter BP, Sheth S, Ramenghi U *et al*. Diagnosing and treating Diamond Blackfan anaemia: results of an international clinical consensus conference. *Br J Haematol* 2008; **142**: 859–876.
- Willig TN, Niemeyer CM, Leblanc T, Tiemann C, Robert A, Budde J *et al*. Identification of new prognosis factors from the clinical and epidemiologic analysis of a registry of 229 Diamond-Blackfan anemia patients. DBA group of Societe d'Hematologie et d'Immunologie Pédiatrique (SHIP), Gesellschaft für Padiatrische Onkologie und Hamatologie (GPOH), and the European Society for Pediatric Hematology and Immunology (ESPHI). *Pediatr Res* 1999; **46**: 553–561.
- Naria A, Vlachos A, Nathan DG. Diamond blackfan anemia treatment: past, present and future. *Sem Hematol* 2011; **48**: 117–123.
- Drapchinskaja N, Gustavsson P, Andersson B, Pettersson M, Willig TN, Dianzani I *et al*. The gene encoding ribosomal protein S19 is mutated in Diamond-Blackfan anaemia. *Nat Genet* 1999; **21**: 169–175.
- Gazda HT, Grabowska A, Merida-Long LB, Latawiec E, Schneider HE, Lipton JM *et al*. Ribosomal protein S24 gene is mutated in Diamond-Blackfan anemia. *Am J Hum Genet* 2006; **79**: 1110–1118.
- Cmejla R, Cmejlova J, Handrkova H, Petrak J, Pospisilova D. Ribosomal protein S17 gene (RPS17) is mutated in Diamond-Blackfan anemia. *Hum Mutat* 2007; **28**: 1178–1182.
- Cmejla R, Cmejlova J, Handrkova H, Petrak J, Petrylova K, Mihal V *et al*. Identification of mutations in the ribosomal protein L5 (RPL5) and ribosomal protein L11 (RPL11) genes in Czech patients with Diamond-Blackfan anemia. *Hum Mutat* 2009; **30**: 321–327.
- Gazda HT, Sheen MR, Vlachos A, Choessel V, O'Donohue MF, Schneider H *et al*. Ribosomal protein L5 and L11 mutations are associated with cleft palate and abnormal thumbs in Diamond-Blackfan anemia patients. *Am J Hum Genet* 2008; **83**: 769–780.
- Quarello P, Garelli E, Carando A, Brusco A, Calabrese R, Dufour C *et al*. Diamond-Blackfan anemia: genotype-phenotype correlations in Italian patients with RPL5 and RPL11 mutations. *Haematologica* 2009; **95**: 206–213.
- Farrar JE, Nater M, Caywood E, McDevitt MA, Kowalski J, Takemoto CM *et al*. Abnormalities of the large ribosomal subunit protein, Rpl35a, in Diamond-Blackfan anemia. *Blood* 2008; **112**: 1582–1592.
- Doherty L, Sheen MR, Vlachos A, Choessel V, O'Donohue MF, Clinton C *et al*. Ribosomal protein genes RPS10 and RPS26 are commonly mutated in Diamond-Blackfan anemia. *Am J Hum Genet* 2010; **86**: 222–228.
- Farrar JE, Vlachos A, Atsidaftos E, Carlson-Donohoe H, Markello TC, Arceci RJ *et al*. Ribosomal protein gene deletions in Diamond-Blackfan anemia. *Blood* 2011; **118**: 6943–6951.
- Choessel V, Bacqueville D, Rouquette J, Noaillic-Depeyre J, Fribourg S, Cretien A *et al*. Impaired ribosome biogenesis in Diamond-Blackfan anemia. *Blood* 2007; **109**: 1275–1283.

14. Choessel V, Fribourg S, Aguisa-Toure AH, Pinaud N, Legrand P, Gazda HT *et al*. Mutation of ribosomal protein RPS24 in Diamond-Blackfan anemia results in a ribosome biogenesis disorder. *Hum Mol Genet* 2008; **17**: 1253–1263.
15. Idol RA, Robledo S, Du HY, Crimmins DL, Wilson DB, Ladenson JH *et al*. Cells depleted for RPS19, a protein associated with Diamond Blackfan Anemia, show defects in 18S ribosomal RNA synthesis and small ribosomal subunit production. *Blood Cells Mol Dis* 2007; **39**: 35–43.
16. Leger-Silvestre I, Caffrey JM, Dawaliby R, Alvarez-Arias DA, Gas N, Bertolone SJ *et al*. Specific Role for yeast homologs of the Diamond Blackfan anemia-associated Rps19 protein in ribosome Synthesis. *J Biol Chem* 2005; **280**: 38177–38185.
17. Ellis SR, Gleizes PE. Diamond blackfan anemia: ribosomal proteins going rogue. *Sem Hematol* 2011; **48**: 89–96.
18. Chakraborty A, Uechi T, Higa S, Torihara H, Kenmochi N. Loss of ribosomal protein L11 affects zebrafish embryonic development through a p53-dependent apoptotic response. *PLoS One* 2009; **4**: e4152.
19. Danilova N, Sakamoto KM, Lin S. Ribosomal protein S19 deficiency in zebrafish leads to developmental abnormalities and defective erythropoiesis through activation of p53 protein family. *Blood* 2008; **112**: 5228–5237.
20. Devlin EE, Dacosta L, Mohandas N, Elliott G, Bodine DM. A transgenic mouse model demonstrates a dominant negative effect of a point mutation in the RPS19 gene associated with Diamond-Blackfan anemia. *Blood* 2010; **116**: 2826–2835.
21. McGowan KA, Li JZ, Park CY, Beaudry V, Tabor HK, Sabnis AJ *et al*. Ribosomal mutations cause p53-mediated dark skin and pleiotropic effects. *Nat Genet* 2008; **40**: 963–970.
22. McGowan KA, Mason PJ. Animal models of diamond blackfan anemia. *Sem Hematol* 2011; **48**: 106–116.
23. Uechi T, Nakajima Y, Chakraborty A, Torihara H, Higa S, Kenmochi N. Deficiency of ribosomal protein S19 during early embryogenesis leads to reduction of erythrocytes in a zebrafish model of Diamond-Blackfan anemia. *Hum Mol Genet* 2008; **17**: 3204–3211.
24. Fumagalli S, Di Cara A, Neb-Gulati A, Natt F, Schwemberger S, Hall J *et al*. Absence of nucleolar disruption after impairment of 40S ribosome biogenesis reveals an rpl11-translation-dependent mechanism of p53 induction. *Nat Cell Biol* 2009; **11**: 501–508.
25. Flygare J, Kiefer T, Miyake K, Utsugisawa T, Hamaguchi I, Da Costa L *et al*. Deficiency of ribosomal protein S19 in CD34⁺ cells generated by siRNA blocks erythroid development and mimics defects seen in Diamond-Blackfan anemia. *Blood* 2005; **105**: 4627–4634.
26. Ohene-Abuakwa Y OK, Marius C, Ball SE. Two-phase culture in Diamond Blackfan anemia: localization of erythroid defect. *Blood* 2005; **105**: 243–252.
27. Miyake K, Utsugisawa T, Flygare J, Kiefer T, Hamaguchi I, Richter J *et al*. Ribosomal protein S19 deficiency leads to reduced proliferation and increased apoptosis but does not affect terminal erythroid differentiation in a cell line model of Diamond-Blackfan anemia. *Stem Cells (Dayton, Ohio)* 2008; **26**: 323–329.
28. Kuramitsu M, Hamaguchi I, Takuo M, Masumi A, Momose H, Takizawa K *et al*. Deficient RPS19 protein production induces cell cycle arrest in erythroid progenitor cells. *Br J Haematol* 2008; **140**: 348–359.
29. Badhai J, Frojmark AS, J Davey E, Schuster J, Dahl N. Ribosomal protein S19 and S24 insufficiency cause distinct cell cycle defects in Diamond-Blackfan anemia. *Biochim Biophys Acta* 2009; **1792**: 1036–1042.
30. Dutt S, Narla A, Lin K, Mullally A, Abayasekara N, Megerdichian C *et al*. Haploinsufficiency for ribosomal protein genes causes selective activation of p53 in human erythroid progenitor cells. *Blood* 2011; **117**: 2567–2576.
31. Dai MS, Lu H. Inhibition of MDM2-mediated p53 ubiquitination and degradation by ribosomal protein L5. *J Biol Chem* 2004; **279**: 44475–44482.
32. Dai MS, Shi D, Jin Y, Sun XX, Zhang Y, Grossman SR *et al*. Regulation of the MDM2-p53 pathway by ribosomal protein L11 involves a post-ubiquitination mechanism. *J Biol Chem* 2006; **281**: 24304–24313.
33. Horn HF, Vousden KH. Cooperation between the ribosomal proteins L5 and L11 in the p53 pathway. *Oncogene* 2008; **27**: 5774–5784.
34. Dai MS, Zeng SX, Jin Y, Sun XX, David L, Lu H. Ribosomal protein L23 activates p53 by inhibiting MDM2 function in response to ribosomal perturbation but not to translation inhibition. *Mol Cell Biol* 2004; **24**: 7654–7668.
35. Yadavilli S, Mayo LD, Higgins M, Lain S, Hegde V, Deutsch WA. Ribosomal protein S3: A multi-functional protein that interacts with both p53 and MDM2 through its KH domain. *DNA Repair* 2009; **8**: 1215–1224.
36. Chen D, Zhang Z, Li M, Wang W, Li Y, Rayburn ER *et al*. Ribosomal protein S7 as a novel modulator of p53-MDM2 interaction: binding to MDM2, stabilization of p53 protein, and activation of p53 function. *Oncogene* 2007; **26**: 5029–5037.
37. Brummelkamp TR, Bernards R, Agami R. A system for stable expression of short interfering RNAs in mammalian cells. *Science* 2002; **296**: 550–553.
38. Naldini L, Blomer U, Gally P, Ory D, Mulligan R, Gage FH *et al*. In vivo gene delivery and stable transduction of nondividing cells by a lentiviral vector. *Science* 1996; **272**: 263–267.
39. Da Costa L, Narla G, Willig TN, Peters LL, Parra M, Fixler J *et al*. Ribosomal protein S19 expression during erythroid differentiation. *Blood* 2003; **101**: 318–324.
40. Angelini M, Cannata S, Mercaldo V, Gibello L, Santoro C, Dianzani I *et al*. Missense mutations associated with Diamond-Blackfan anemia affect the assembly of ribosomal protein S19 into the ribosome. *Hum Mol Genet* 2007; **16**: 1720–1727.



Cell Death and Disease is an open-access journal published by **Nature Publishing Group**. This work is licensed under the **Creative Commons Attribution-NonCommercial-NoDerivative Works 3.0 Unported License**. To view a copy of this license, visit <http://creativecommons.org/licenses/by-nc-nd/3.0/>

Supplementary Information accompanies the paper on Cell Death and Disease website (<http://www.nature.com/cddis>)